Chemistry–A European Journal

Research Article
doi.org/10.1002/chem.202403005

Chemistry Europe
European Chemical Societies Publishing

www.chemeurj.org

Substitution of the Axial Type 1 Cu Ligand Affords Binding of a Water Molecule in Axial Position Affecting Kinetics, Spectral, and Structural Properties of the Small Laccase Ssl1

Anna C. Olbrich[+],[a] Steffen Mielenbrink[+],[b] Vivian P. Willers,[a] Katja Koschorreck,[a] James A. Birrell,[c] Ingrid Span,*[b, d] and Vlada B. Urlacher*[a]

Multicopper oxidases use Cu ions as cofactors to oxidize various substrates. High reduction potential at Type 1 Cu is considered as crucial for effective catalysis. Previous studies have shown that replacing the axial methionine ligand of the Type 1 Cu with leucine or phenylalanine leads to an increased reduction potential, but not always to higher enzyme activity. Here we present a study on six variants of the small laccase Ssl1 from *Streptomyces sviceus*, where the axial methionine ligand was substituted, and the effect of the axial ligand on reduction potential, activity, spectral properties and structure was investigated. Absorption, electronic circular dichroism and EPR spectra revealed the presence of a stronger coordinating axial ligand like oxygen, which influences the electronic and catalytic properties more than the nature of the amino acid side chain. The crystal structures of the Ssl1 variants were solved, which show that none of the amino acid side chains coordinate to the Cu. Instead, a water molecule is found in the axial coordination site, which support the spectroscopic data. Our findings highlight the importance of combining structural and spectroscopic methods to investigate the effect of amino acid exchange on multicopper oxidases.

Introduction

Multicopper oxidases (MCOs) build a diverse group of enzymes that catalyze the one-electron oxidation of organic compounds by the four-electron reduction of molecular oxygen to water.[1] MCOs have emerged as attractive biocatalysts that accept (poly)phenols, amines, and other substrates and enable their oxidation and subsequent C–C, C–O, and C–N coupling.[2] These enzymes have also been used for bioremediation, delignification of lignocellulose, and in biofuel cells.[3] MCOs typically contain four copper ions, arranged in one mononuclear type 1 copper (T1 Cu) site and a trinuclear copper cluster (TNC), composed of one mononuclear type 2 copper (T2 Cu) and a hydroxo bridged, antiferromagnetically coupled, binuclear type 3 copper (T3 Cu) site.[4] Electrons are transferred from the substrate to the T1 Cu and from the T1 Cu via a superexchange pathway to the TNC where O_2 binding and reduction occurs.[5]

One of the most important characteristics of MCOs for effective catalysis is the reduction potential (E°) of their T1 Cu ($E^{\circ\prime}$T1Cu), as these enzymes can only oxidize compounds whose E° is not much higher than their own E°.[6] Kinetic studies on laccases with several substrates demonstrated that the reaction rates correlated with the difference between the reduction potentials of the T1 Cu and the respective substrate (ΔE).[7]

The T1 Cu is coordinated by at least three ligands, one cysteine and two histidine residues in a pseudo-trigonal manner, and the variations in T1 Cu sites in different MCOs arise from different axial ligands.[8] While azurin and plastocyanin have a single Cu ion coordinated by the axial methionine ligand in a trigonally distorted tetrahedral geometry, considered classic blue copper site, there are many copper proteins with "perturbed" blue copper (T1) sites.[9] Among those are copper proteins like stellacyanin, in which the axial methionine is replaced by a stronger coordinating glutamine.[10] "Perturbed" copper sites are also reported for fungal laccases in which the axial methionine is replaced with non-coordinating leucine or phenylalanine.[11]

Fungal laccases, with a non-coordinating axial leucine or phenylalanine, exhibit high activities and accept a broad range of substrates, both attributed to the high $E^{\circ\prime}$T1Cu of up to +800 mV.[6,12] Their application is however limited by the preference for acidic pH and the susceptibility towards

[a] A. C. Olbrich,[+] V. P. Willers, K. Koschorreck, V. B. Urlacher
Institute of Biochemistry, Heinrich Heine University Düsseldorf, Universitätsstr. 1, Düsseldorf 40225, Germany
E-mail: Vlada.Urlacher@uni-duesseldorf.de

[b] S. Mielenbrink,[+] I. Span
Institut für Physikalische Biologie, Heinrich Heine University Düsseldorf, Universitätsstr. 1, Düsseldorf 40225, Germany

[c] J. A. Birrell
School of Life Sciences, University of Essex, Wivenhoe Park, Colchester CO4 3SQ, UK

[d] I. Span
Bioinorganic Chemistry, Friedrich-Alexander-Universität Erlangen-Nürnberg, Egerlandstr. 1, Erlangen 91058, Germany
E-mail: Ingrid.Span@fau.de

[+] These authors contributed equally

Supporting information for this article is available on the WWW under https://doi.org/10.1002/chem.202403005

inhibitors.[13] In contrast, their bacterial counterparts remain active at neutral and even alkaline pH. They also display an exceptional stability at elevated temperatures and at high concentrations of organic solvents.[14] The main drawback of bacterial laccases is their lower activity and narrower substrate spectrum compared to fungal laccases. This is mainly attributed to the presence of the axial methionine coordinating the T1 Cu, resulting in lower $E^{\circ\prime}$T1Cu of +300 to +400 mV. Replacement of the axial methionine by non-coordinating leucine or phenylalanine as well as substitutions in the second coordination sphere of T1 Cu increased $E^{\circ\prime}$T1Cu in several MCOs.[3a,15]

In our previous study, we applied site-specific mutagenesis at positions in the first and second T1 Cu coordination sphere to convert the low-redox potential small two-domain laccase Ssl1 from *Streptomyces sviceus* ($E^{\circ\prime}$T1Cu = +375 mV) into a MCO with $E^{\circ\prime}$T1Cu of up to +560 mV.[16] Essential changes in $E^{\circ\prime}$T1Cu were achieved by replacing the axial methionine at position 295 with one of the non-coordinating amino acids alanine, valine, threonine, phenylalanine, tyrosine or isoleucine.[16] The Ssl1 variants with $E^{\circ\prime}$T1Cu of $\geq$ +500 mV enabled oxidation of substrates not oxidizable by the wild-type enzyme (WT).[16–17] However, not all Ssl1 variants with increased $E^{\circ\prime}$T1Cu demonstrated enhanced activities towards certain substrates like alizarin red S (+790 mV) and even syringaldazine (+390 mV).[16] Other factors like effects from substrate structure,[18] substrate binding[19] and structural changes need to be considered as well. Currently, there are much less structural data on two-domain bacterial laccases and their variants available compared to fungal three-domain laccases. For the Ssl1 WT and the Ssl1 M295L variant crystal structures were solved by our group, while other groups determined the crystal structures of several variants of a small two-domain laccase from *Streptomyces coelicolor* and *S. griseoflavus* Ac-993.[15c,20]

In this study, the electronic and structural properties of six Ssl1 variants with non-coordinating axial ligands, alanine, valine, threonine, phenylalanine, tyrosine or isoleucine, were investigated. We studied the influence of the axial ligand on the $E^{\circ\prime}$T1Cu values, T1 Cu reduction kinetics, electronic absorption, electronic circular dichroism (ECD) and electron paramagnetic resonance (EPR) spectra. To rationalize the observed differences and to gain a deeper insight into the geometry of the T1 Cu sites, we solved and analyzed the crystal structures of the Ssl1 axial ligand variants.

Results and Discussion

First, we investigated the relation between the rate of intermolecular electron transfer (ET) from a substrate to T1 Cu (k_{ET} of T1 Cu reduction) and the $E^{\circ\prime}$T1Cu in Ssl1 variants using the common low-redox potential laccase substrate hydroquinone (HQ).[21] In order to disrupt the intramolecular ET from the T1 Cu to the TNC, and thereby focus on the ET from HQ to the T1 Cu, we constructed T2 Cu depleted (T2D) Ssl1 variants. To this end, His99 was replaced by tyrosine, preventing T2 Cu coordination, as previously reported for the MCO FET3 from *Saccharomyces cerevisiae*.[22] The $E^{\circ\prime}$T1Cu of the T2D Ssl1 variants (Table 1, Figures S1–S7) were in good agreement with values previously reported by our group for the corresponding Ssl1 variants with an intact T2 Cu.[16] One-electron transfer from HQ to the T1 Cu was analyzed using a stopped-flow approach. The decrease in absorption at ~600 nm that accompanies the reduction of the T1 Cu^{II} upon HQ oxidation followed a first order exponential decay in T2D Ssl1 variants (Figures S8–S14, Tables S1–S7) as was reported for the *Rhus vernicifera* laccase depleted in T2 Cu.[23] The measured k_{ET} values varied over two orders of magnitude between the fastest reduction in the T2D Ssl1 variant with axial methionine (k_{ET} = 2.01 s^{-1}) and the slowest measured with the Ssl1 M295A T2D variant (k_{ET} = 0.02 s^{-1}) (Table 1). As expected, the k_{ET} values correlated with the $E^{\circ\prime}$T1Cu in the series of the constructed variants, where more negative potentials give lower k_{ET} values and more positive potentials give higher k_{ET} values. However, even though the M295V, M295F, and M295I variants have higher $E^{\circ\prime}$T1Cu than the Ssl1 variant with axial methionine, their k_{ET} values were lower (Table 1). According to Marcus theory, k_{ET} is influenced not only by the free energy difference ΔG°, which is directly related to the reduction potential difference ΔE, but also by the reorganization energy λ, and the donor-acceptor electronic coupling H_{DA}.[24]

Our observations suggest that the substitutions caused changes not only in $E^{\circ\prime}$T1Cu but also in the reorganization energy and/or electronic coupling. Interestingly, for the recently reported mutants of another small laccase SLAC, substitutions in the second T1 Cu coordination sphere led to an increase in $E^{\circ\prime}$T1Cu of up to +190 mV, while k_{cat}, which can be correlated to k_{ET}, decreased for most of the variants.[15c]

Spectral properties of the Ssl1 variants were investigated by electronic absorption and ECD spectroscopies (Figures 1 and S15, Tables S8–S10). Ssl1 WT has spectral characteristics of a typical laccase with an intense absorption band at around 590 nm, which derives from the charge transfer (CT) S(Cys)$\pi\rightarrow$Cu(II) transition.[20a] Spectral properties of the variants revealed "perturbations". The most intriguing effect of mutations at position 295 on the absorption spectra is the shift from a blue to a green site and appearance of an additional band at ~430 nm, present in all Ssl1 variants (Figure 1, Table S9). The ratio of the two peaks at ~430 nm and ~590 nm was lowest for the M295A and M295V variants and highest for the M295Y,

Table 1. Reduction potentials $E^{\circ\prime}$T1Cu and k_{ET} values of T1 Cu reduction by HQ measured for the T2D Ssl1 variants. Values are given as mean ± standard deviation of at least triplicates.

Ssl1 variant H99Y/	Reduction potential $E^{\circ\prime}$T1Cu [mV]	Reduction rate k_{ET} [s^{-1}]
M295A	< 290	0.02 ± 0.008
M295T	306 ± 13	0.07 ± 0.005
M295Y	396 ± 9	0.37 ± 0.19
M295	404 ± 9	2.01 ± 0.31
M295F	430 ± 9	0.99 ± 0.26
M295V	432 ± 3	0.93 ± 0.17
M295I	442 ± 11	1.40 ± 0.13

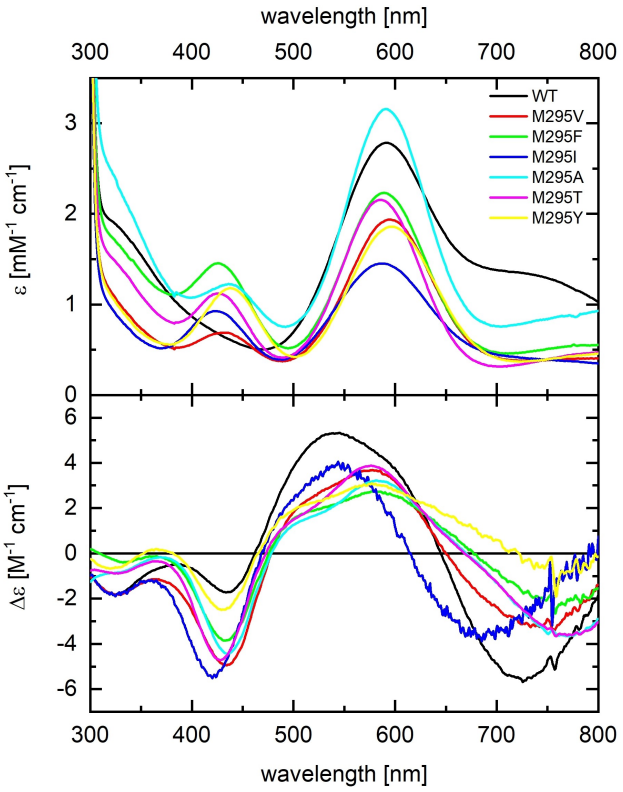

Figure 1. Electronic absorption (top) and ECD (bottom) spectra of Ssl1 WT (black curves) and the variants M295V (red), M295F (green), M295I (dark blue), M295A (light blue), M295T (pink), and M295Y (yellow).

M295I, and M295F variants (Table S9). A similar two-band pattern has been reported and discussed for other MCOs with a stronger axial ligand than methionine (e.g. oxygen from glutamine or glutamate) or where binding of a water molecule was suggested.[25] For instance, the M121E variant of azurin showed a pH-dependent increase at ~400 nm in the electronic absorption spectrum.[26] Similar spectral features have been reported for axial variants of CueO from *Escherichia coli*, which most likely have an O atom occupying the vacant axial position, originating from the respective side chains in the M510Q and M510T variants or from a proposed water molecule in M510A, which was, however, not confirmed by structural data.[25b] Replacing the axial methionine ligand in *Thermus thermophilus* SG0.5JP17-16 laccase by alanine (M460A) resulted also in an additional absorption band at ~440 nm in the electronic absorption spectrum, similar to the Ssl1 variants studied here.[27]

Substitutions of the axial methionine also affected the d-d transitions (mostly $d_{xz}/d_{yz} \rightarrow d_{x^2-y^2}$ from the T1) between 700 and 800 nm in the absorption and ECD spectra. While an increase in ligand field was expected by replacing the axial methionine by a non-coordinating ligand,[28] only for the M295I variant a shift of the d-d transition feature to lower wavelength/higher energy was observed. This could indicate a larger ligand field splitting, increasing the energy of the $d_{x^2-y^2}$, as reported for fungal laccases with non-coordinating axial ligands. In the M295F, M295V, M295Y, M295A, and M295T variants the d-d transitions shifted to higher wavelength/lower energy and were less intense than in Ssl1 WT (Figure 1, Table S10) reflecting a weaker ligand field due to tetrahedral distortion of the T1 Cu site.

Continuous wave (CW) X-band (9.64 GHz) EPR spectra gave further insights into the effects of the mutations on the geometry of the T1 Cu site (Figure 2, Table 2). The EPR spectrum of Ssl1 WT is reminiscent of typical bacterial MCOs with two components, the T1 Cu and T2 Cu site. The first is an axial spectrum ($g_1 = g_\parallel = 2.230$, $(g_2+g_3)/2 = g_\perp = 2.046$) with a small anisotropic hyperfine coupling to the I = 3/2 Cu nucleus ($A_\parallel = 74 \cdot 10^{-4}\,cm^{-1}$ and $A_\perp = 12 \cdot 10^{-4}\,cm^{-1}$) that splits the $g_\parallel$ into four lines.[8b,29] The second component is also axial ($g_\parallel = 2.215$ and $g_\perp = 2.05$), but with a much larger anisotropic Cu hyperfine coupling ($A_\parallel = 200 \cdot 10^{-4}\,cm^{-1}$ and $A_\perp = 1 \cdot 10^{-4}\,cm^{-1}$). This is typical of tetragonal T2 Cu sites with a highly ionic Cu center (low covalency).

By replacing the weakly coordinating axial methionine with non-coordinating ligands, we expected axial EPR spectra similar to those of Ssl1 WT or of fungal laccases lacking a coordinating axial ligand. However, all Ssl1 variants exhibited rhombic EPR spectra where the characteristic T1 Cu site is significantly altered with increased $g_\parallel$-values and reduced $A_\parallel$ values, as observed for copper proteins with stronger axial ligands like glutamine in stellacyanin or in the M121Q mutant of azurin.[30]

The increased rhombicity of the EPR spectra indicates some d_{z^2} mixing into the $d_{x^2-y^2}$ ground state, which is in agreement with the lower energy ligand field transitions observed in the electronic spectra (Figure 1). The increased g_1 value also indicates larger spin-orbit coupling due to mixing of excited states into the $d_{x^2-y^2}$ ground state. These effects are consistent with changes to a more tetrahedral coordination geometry around the T1 Cu site, which affects the level of ligand-metal orbital overlap (see SI for further discussion). Taken together, these results further suggest that water has most likely taken over the role of the axial ligand, thereby influencing the T1 Cu site geometry, as supported by the EPR spectra. Due to more

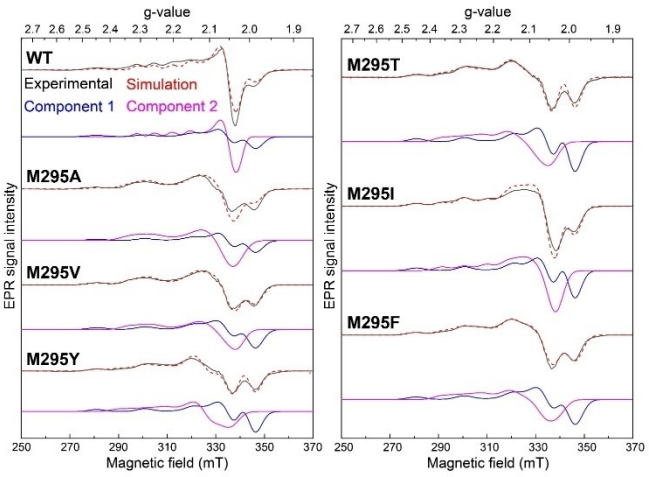

Figure 2. Continuous wave (cw) X-band (9.63 GHz) EPR spectra of 0.2–0.6 mM samples of Ssl1 WT and the variants M295A, M295V, M295Y, M295T, M295I, and M295F (black lines) along with simulations (red dashed lines). The two components in the simulation are shown beneath in blue and pink lines. EPR spectra were measured at 30 K.

Table 2. EPR parameters of the T1 Cu site in the Ssl1 WT and variants. Copper hyperfine coupling constant A is given in x 10^{-4} cm^{-1} . $g_\perp$ is the average of g_2 and g_3. $g_1 = g_\parallel$. Literature data for stellacyanin[9] and azurin M121Q[39] are provided for comparison.

Ssl1 variant	T1								T2						Ratio T1/T2
	g_1	g_2	g_3	$g_\perp$	η[a]	A_1	A_2	A_3	g_1	g_2	g_3	A_1	A_2	A_3	
WT	**2.230**	2.059	2.033	2.046	0.21	**74**	13	10	**2.215**	2.050	2.050	**200**	1	1	1
M295F	**2.298**	2.108	2.040	2.074	0.46	**60**	33	20	**2.216**	2.050	2.050	**200**	13	13	1
M295V	**2.298**	2.075	2.050	2.063	0.16	**43**	40	20	**2.214**	2.050	2.050	**198**	13	13	1
M295Y	**2.300**	2.120	2.050	2.085	0.49	**67**	13	13	**2.215**	2.050	2.050	**200**	13	13	1
M295I	**2.255**	2.075	2.045	2.060	0.23	**93**	30	13	**2.215**	2.050	2.050	**200**	13	13	1
M295A	**2.298**	2.075	2.050	2.063	0.16	**43**	33	13	**2.215**	2.050	2.050	**200**	1	1	1
M295T	**2.298**	2.120	2.050	2.085	0.49	**60**	28	13	**2.215**	2.050	2.050	**200**	13	13	1
Stellacyanin[9]	**2.290**	2.080	2.030	2.055	0.32	**35**	n.r.[b]	n.r.[b]	–	–	–	–	–	–	–
Azurin M121Q[39]	**2.287**	2.077	2.025	2.051	0.33	**35**	29	57	–	–	–	–	–	–	–

[a] Rhombicity: $(g_2-g_3)/(g_1-g_{av})$, where $g_{av}=(g_1+g_2+g_3)/3$. [b] A_2 and A_3 are too small to be reliably estimated.

space at the axial position of the T1 Cu the coordination site can form a more tetrahedral geometry.

As expected, EPR spectroscopy showed that the T2 Cu site of the constructed variants was not affected by the amino acid substitutions.

To elucidate the structural changes that occurred in the Ssl1 variants and to interpret our findings from kinetic measurements and spectral analyses, we solved the structures of five Ssl1 variants M295A, M295Y, M295F, M295V, and M295I (Figure 3, Figure S16 and Table S11). No crystals could be obtained for the M295T variant after several attempts. The overall architecture of all Ssl1 variants is very similar to the WT structure (PDB ID 4M3H) and the Ssl1 M295L variant (PDB ID 4WTQ) with root mean square deviations (RMSD) in the range of 0.330–0.599 Å (calculated for all Cα atoms of residues 43–311 without outlier rejection). The electron density of the exchanged amino acids at position 295 revealed that none of the side chains directly interacts with the T1 Cu. The side chains of alanine, isoleucine, and valine in the respective variants M295A, M295I, and M295V, are well defined, however, they are too

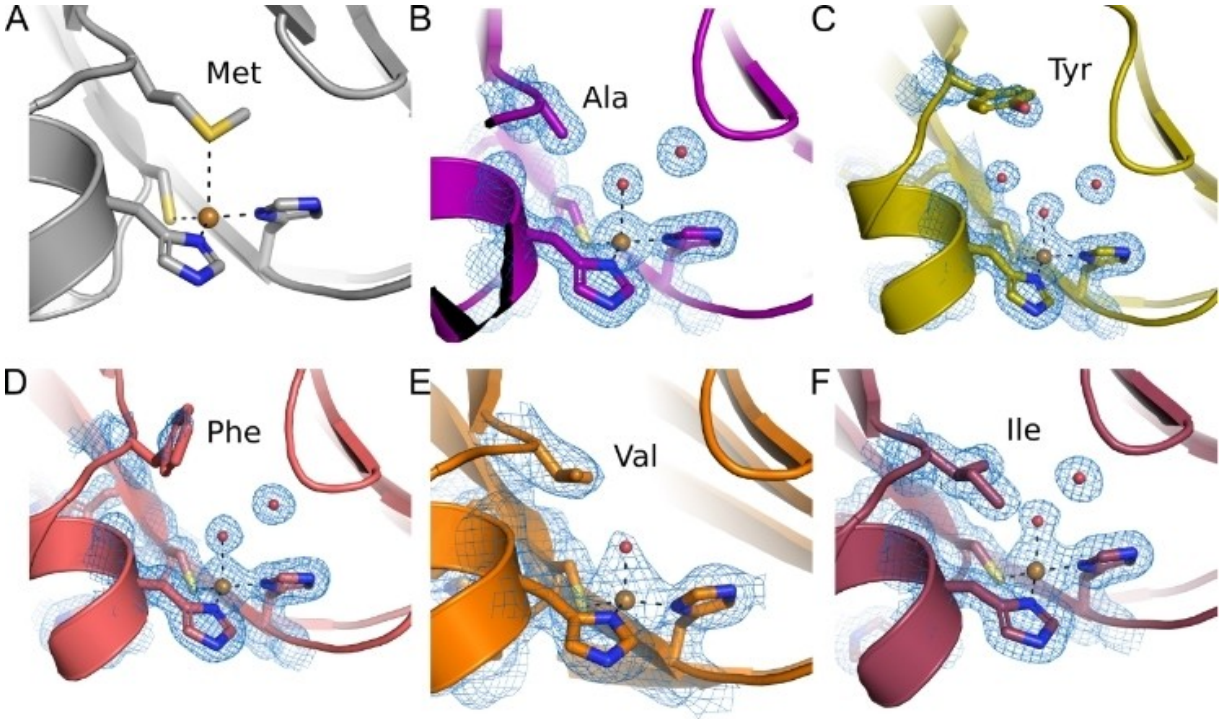

Figure 3. Structure of the T1 Cu sites of the Ssl1 WT (A) and the Ssl1 variants M295A (B), M295Y (C), M295F (D), M295V (E), and M295I (F). The protein backbone is shown as cartoon and the amino acids side chains are shown as sticks with the atoms colored according to the color code: N in blue and S in yellow. The T1 Cu atoms are shown as orange spheres, and the oxygen atoms of water molecules are represented as red spheres. A $2F_O$-F_C electron density map (blue mesh, contoured at 1 σ) is shown for the T1 Cu, the residues in the first coordination sphere of the T1 Cu, the residue at position 295, and water molecules in close proximity to the copper ion. The mutation H99Y was not introduced in these variants.

short and do not have atoms capable of forming bonds with the T1 Cu. The larger residues F295 and Y295 are not well defined, and the electron density indicates that the side chains are flipped away from the T1 Cu site.

As indicated by our spectral analyses, a trigonal, three-coordinated T1 Cu, lacking a fourth axial ligand is not afforded in the constructed variants. Instead, in the structures of all Ssl1 variants one or two additional well-defined water molecules were observed in the pocket, which is occupied by methionine in Ssl1 WT, where no water was observed. Interestingly, the amino acid exchange not only allowed water molecules to enter the pocket, but also influenced the stability of the loop located near position 295. The region around 203–205 is disordered, suggesting higher flexibility in the variants. Taken together, the side chains of residue 295 in the five variants do not reach all the way into the pocket and are not capable of interacting with the T1 Cu, while a water occupied the open coordination site (Figure 4).

The T1 Cu site in Ssl1 WT has a trigonally distorted tetrahedral structure with the Cu ion coordinated by four ligands. The trigonal plane contains a Cu ion with two almost equal Cu–N(His) distances, and an equatorial S(Cys) ligand with a Cu–S(Cys) bond length of 2.1 Å (Figure 3A, Table S12) similar to classic blue copper proteins.[9] The replacement of the axial methionine and introduction of a water molecule decreased the distortion of the tetrahedron, which was confirmed by crystallographic data giving more tetrahedral structures with smaller total Cu-ligand angles in the constructed variants and T1 Cu moving more out of plane (Figure 4, Table S13). Thereby, the Cu–S(Cys) distance was slightly more affected than the Cu–N(His) distance (Table S14).

The Cu–S(Cys) bond in almost all variants was increased, with the largest differences between WT and the M295V and M295Y variants. The Cu–N(His) distances in Ssl1 variants remained predominantly within a 0.01–0.07 Å range of each other (Table S14).

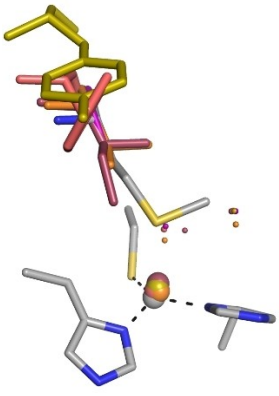

Figure 4. Superposition of the axial ligands at the T1 Cu site of Ssl1 WT and variants. WT in gray, A295 in magenta, Y295 in olive, F295 in light red, V295 in orange, and I295 in dark red. The residues in the first coordination sphere of the T1 Cu in the WT structure are shown as sticks with the atoms colored according to the color code: C in gray, N in blue, and S in yellow. The T1 Cu atoms are shown as larger spheres, water molecules are shown as smaller spheres, and colored in the same color as the axial ligand.

Stretching of the Cu–S(Cys) bond when switching from a weakly coordinated axial ligand like methionine to more strongly coordinated ones like glutamine has been reported for several copper proteins.[9,25b] However, binding of a water molecule in the axial position of T1 Cu confirmed by crystallographic data has only been rarely reported, e.g. for the M121G variant of azurin, while in the M121A variant water was not present, as for the M98A variant of amicyanin.[31] Literature data on the substitution of the axial methionine by non-coordinating ligands in bacterial laccases are not consistent. Some of them did not describe any indication for the binding of a water molecule in the axial position.[15a,20b,27] For the M460A variant of *T. thermophilus* SG0.5JP17-16 laccase and the M510A variant of bacterial laccase CueO from *E. coli* the presence of a water molecule was suggested on the basis of spectral data, but this was not confirmed by crystallographic data.[15b,27] Thus, to the best of our knowledge we report for the first time on binding of a water molecule in the axial position of T1 Cu in MCO variants with non-coordinating axial ligands, evidenced by spectroscopic and crystallographic data.

The crystal structures further show higher solvent access to the T1 Cu site in M295A compared to M295V (Figure 3), which might explain the large differences in both $E^{\circ\prime}$T1Cu and k_{ET} values of both variants. Furthermore, the M295A variant shows a much larger decrease in energy for the ligand-field transition (absorption at 767 nm) than the M295V variant (absorption at 738 nm), indicating a larger tetrahedral distortion for the former variant. It seems likely that this would be due to electrostatic effects, i.e., differences in the hydrophobicity of the local T1 Cu environment. Similar observations were made previously with azurin.[32] Solvent accessibility also influences the reorganization energy, as was recently demonstrated by the correlation between the solvent accessible surface area and the reorganization energy using a series of engineered T1 Cu sites.[33]

The spectroscopic data characteristic for a tetrahedral distortion of the T1 Cu site indicate an increase in reorganization energy for the Cu(II) to Cu(I) reduction in Ssl1 variants with axial ligands other than methionine. According to the Rack/entatic state theory,[11a,34] the protein environment, specifically, the axial ligand enforces a slightly unfavorable geometry of the Cu ion, but one that is close to the transition state structure during reduction/oxidation. Replacement of the axial methionine by water allows the T1 Cu to relax into a state with locally lower energy but with a larger reorganization energy. Generally, the reorganization energy λ is energy required to reorganize reactant bonds and surrounding solvent to match those found in the product, before ET occurs.[35] The impact of the axial ligand on the reorganization energy was previously demonstrated for several T1 Cu sites.[36] For the M150G and M150W mutants of a nitrite reductase (NiR), the reorganization energy of the T1 Cu was 0.3 eV (30 kJ mol^{-1}) higher than in the NiR wild-type.[36a] Both NiR variants possessed higher T1 Cu midpoint potentials. The rates of the T1 Cu reduction also changed, but were dependent on the electron donor.[36a] The contribution of the reorganization energy to the activation energy is not simple. If the reorganization energy is larger than the free energy change of the reaction, the activation energy

will decrease with decreasing reorganization energy. The activation energy is lowest and the ET rates are fastest if the free energy change matches the negative value of the reorganization energy. If the reorganization energy is equal to or less than the free energy change, reducing the reorganization energy leads to slower ET rates. Several azurin variants with mutations in the outer coordination sphere of T1 Cu demonstrated up to 10-fold higher intramolecular ET rates than the wild-type, because they have lower reorganization energies.[37] While these azurin variants showed ET rates close to a maximum value, other azurin variants with lower reorganization energy showed much lower ET rates.[38] This reduction in reorganization energy was attributed to higher flexibility of their T1 Cu sites.[37] Thus, the lower k_{ET} values measured in this study with the Ssl1 variants with increased $E^{\circ\prime}$T1Cu seem to be due to the higher reorganization energy.

Another factor that can also affect the k_{ET} values is the donor-acceptor electronic coupling matrix element H_{DA} of Marcus theory, which for the ET between the substrate and the T1 Cu in laccases is mainly determined by the short distance between them.[1a] Since our attempts to co-crystallize Ssl1 with the substrate failed, we compared the putative binding sites of the Ssl1 WT and variants. As reported in our previous work, two methionine residues, M195 and M293, located near T1Cu and close to the enzyme surface, form two opposite ridges of the putative substrate binding site.[20a] No significant differences were found for the position of M195 compared to the wild type, whereas visible deviations were observed for the position of M293 in the variants (Figure 5).

In all Ssl1 variants the M293 side chain clusters with the sulfur atom in the precisely same position, in the wild type this side chain is in a completely different orientation. Comparison of the surface area at the putative binding site shows that the altered conformation of the M293 side chain leads to changes of this surface area (Figure S17). These changes impact the accessibility of the substrate binding site. Thus, while increased reorganization energy is most likely the main factor affecting the ET rates from the substrate to T1 Cu, we cannot rule out the possibility that differences in donor-acceptor coupling may also play a role, because the observed subtle structural differences on the protein surface of the variants may influence the exact mode of substrate binding. However, further investigation of this aspect will require solving additional structures in the presence of substrate.

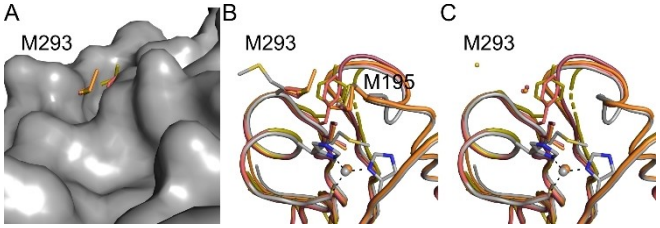

Figure 5. Structural changes at the putative substrate binding site of Ssl1 WT and variants. A) The surface of Ssl1 WT is shown in gray and the side chains of residues 293 and 295 are shown according to the color code. B) Structural superpositions with the side chains of residues at positions 195, 293, and 295 are shown as sticks. The Cu ions are shown as spheres and the dashed lines indicate the coordination of the metal. C) The sulfur atom of M293 is shown as sphere to highlight the different position of the residue in WT compared to the variants. Ssl1 WT is shown in gray, the variants in different colors, according to the following color code: M295A (magenta), M295Y (olive), M295F (light red), M295V (orange), and M295I (dark red).

Conclusions

In summary, we have shown that the exchange of the axial ligand of the T1 Cu site in the small laccase Ssl1 by several non-coordinating amino acids results in binding of a water molecule in the axial position, influencing $E^{\circ\prime}$T1Cu and k_{ET} values. This should be considered in further mutagenesis studies on laccases and other MCOs, aiming at increasing $E^{\circ\prime}$T1Cu and k_{ET}. While axial variants in various MCOs and Cu proteins have been extensively studied using different spectroscopic methods, in most cases no supporting structural data were available. Our study provides experimental evidence that replacement of the axial ligand leads to displacement of amino acids from the first coordination sphere of Ssl1, allowing water to occupy the open coordination site. The observed properties are characteristic for "perturbed" T1 Cu sites with an oxygen donor ligand bound to the T1 Cu in the axial position such as in stellacyanin with axial glutamine[9] and the M121Q mutant of azurin,[39] even though the origin of the coordinating oxygen donor ligand differs (amide vs water). The combined analysis of the structural and electronic properties of a series of axial Ssl1 variants allow us to suggest that the presence of an oxygen donor ligand in the first coordination sphere of the Cu ion has a stronger influence on the electronic properties and activity than the chemical properties of the introduced amino acid side chains. The availability of crystal structures to complement the spectroscopic data therefore provides unique insights into the structure-activity relationship. These findings are of crucial importance for understanding the properties of T1 Cu sites and for the rational design of biocatalysts.

Supporting Information Summary

The data supporting the results of this study including experimental procedures are available in the Supporting Information. The authors have cited additional references within the Supporting Information.[40]

Acknowledgements

We acknowledge DESY (Hamburg, Germany), a member of the Helmholtz Association HGF, for the provision of experimental facilities. Parts of this research were carried out at PETRA III and we would like to thank Johanna Hakanpää and Guillaume Pompidor for assistance in using beamline P11. Beamtime was allocated for proposal I-20190878. We also acknowledge George E. Cutsail Max Planck Institute for Chemical Energy Conversion in Mülheim a.d. Ruhr, Germany, for assistance with data

collection. Open Access funding enabled and organized by Projekt DEAL.

Conflict of Interests

The authors declare no conflict of interest.

Data Availability Statement

The data that support the findings of this study are available from the corresponding author upon reasonable request.

Keywords: Laccase · Reduction potential · Type I copper · Axial ligand · Crystal structure

[1] a) S. M. Jones, E. I. Solomon, *Cell. Mol. Life Sci.* **2015**, *72*, 869; b) E. I. Solomon, *Inorg. Chem.* **2016**, *55*, 6364; c) E. I. Solomon, D. E. Heppner, E. M. Johnston, et al., *Chem. Rev.* **2014**, *114*, 3659.
[2] a) M. D. Cannatelli, A. J. Ragauskas, *Chem. Rec.* **2017**, *17*, 122; b) C. Jager, M. Haase, K. Koschorreck, et al., *Angew. Chem. Int. Ed. Engl.* **2023**, *62*, e202213671; c) M. Kawaguchi, T. Ohshiro, M. Toyoda, et al., *Angew. Chem. Int. Ed. Engl.* **2018**, *57*, 5115; d) S. Obermaier, W. Thiele, L. Furtges, et al., *Angew. Chem. Int. Ed. Engl.* **2019**, *58*, 9125; e) A. C. Sousa, M. C. Oliveira, L. O. Martins, et al., *Adv. Synth. Catal.* **2018**, *360*, 575.
[3] a) C. D. Dong, A. Tiwari, G. S. Anisha, et al., *Environ. Pollut.* **2023**, *319*, 120999; b) A. Le Goff, M. Holzinger, S. Cosnier, *Cell. Mol. Life Sci.* **2015**, *72*, 941; c) P. Lopes, K. Koschorreck, J. N. Pedersen, et al., *Chemelectrochem* **2019**, *6*, 2043; d) N. Mano, A. de Poulpiquet, *Chem. Rev.* **2018**, *118*, 2392; e) D. Rodriguez-Escribano, F. de Salas, R. Pliego, et al., *Polymers (Basel)* **2023**, *15*; f) L. Zhang, H. Cui, Z. Zou, et al., *Angew. Chem. Int. Ed. Engl.* **2019**, *58*, 4562.
[4] E. I. Solomon, M. J. Baldwin, M. D. Lowery, *Chem. Rev.* **1992**, *92*, 521.
[5] a) O. Farver, I. Pecht, *Coord. Chem. Rev.* **2011**, *255*, 757; b) S. J. George, M. D. Lowery, E. I. Solomon, et al., *J. Am. Chem. Soc.* **1993**, *115*, 2968; c) A. Sekretareva, S. Tian, S. Gounel, et al., *J. Am. Chem. Soc.* **2021**, *143*, 17236.
[6] A. Sekretaryova, S. M. Jones, E. I. Solomon, *J. Am. Chem. Soc.* **2019**, *141*, 11304.
[7] F. Xu, *Biochemistry* **1996**, *35*, 7608.
[8] a) T. Sakurai, K. Kataoka, *Cell. Mol. Life Sci.* **2007**, *64*, 2642; b) L. Quintanar, M. Gebhard, T.-P. Wang, et al., *J. Am. Chem. Soc.* **2004**, *126*, 6579.
[9] S. DeBeer George, L. Basumallick, R. K. Szilagyi, et al., *J. Am. Chem. Soc.* **2003**, *125*, 11314.
[10] P. J. Hart, A. M. Nersissian, R. G. Herrmann, et al., *Protein Sci.* **1996**, *5*, 2175.
[11] a) L. B. LaCroix, S. E. Shadle, Y. N. Wang, et al., *J. Am. Chem. Soc.* **1996**, *118*, 7755; b) A. M. Nersissian, E. L. Shipp, *Adv. Protein Chem.* **2002**, *60*, 271.
[12] O. V. Morozova, G. P. Shumakovich, M. A. Gorbacheva, et al., *Biochemistry (Mosc.)* **2007**, *72*, 1136.
[13] P. Baldrian, *FEMS Microbiol. Rev.* **2006**, *30*, 215.
[14] a) F. Akram, S. Ashraf, I. U. Haq, et al., *Appl. Biochem. Biotechnol.* **2022**, *194*, 2336; b) P. S. Chauhan, B. Goradia, A. Saxena, *3 Biotech* **2017**, *7*, 323.
[15] a) P. Durao, I. Bento, A. T. Fernandes, et al., *J. Biol. Inorg. Chem.* **2006**, *11*, 514; b) S. Kurose, K. Kataoka, N. Shinohara, et al., *Bull. Chem. Soc. Jpn.* **2009**, *82*, 504; c) J. X. Wang, A. C. Vilbert, C. Cui, et al., *Angew. Chem. Int. Ed. Engl.* **2023**, *62*, e202314019.
[16] A. C. Olbrich, J. N. Schild, V. B. Urlacher, *J. Inorg. Biochem.* **2019**, *201*, 110843.
[17] M. Gunne, V. B. Urlacher, *PLoS One* **2012**, *7*, e52360.
[18] M. A. Tadesse, A. D'Annibale, C. Galli, et al., *Org. Biomol. Chem.* **2008**, *6*, 868.
[19] N. J. Christensen, K. P. Kepp, *J. Mol. Catal. B: Enzym.* **2014**, *100*, 68.
[20] a) M. Gunne, A. Höppner, P. L. Hagedoorn, et al., *FEBS J.* **2014**, *281*, 4307; b) K. Zovo, H. Pupart, A. Van Wieren, et al., *ACS Omega* **2022**, *7*, 6184; c) A. Gabdulkhakov, I. Kolyadenko, O. Kostareva, et al., *Int. J. Mol. Sci.* **2019**, *20*.
[21] S. Steenken, P. Neta, *J. Phys. Chem. A* **1982**, *86*, 3661.
[22] N. J. Blackburn, M. Ralle, R. Hassett, et al., *Biochemistry* **2000**, *39*, 2316.
[23] R. M. Wynn, D. B. Knaff, R. A. Holwerda, *Biochemistry* **1984**, *23*, 241.
[24] R. A. Marcus, N. Sutin, *Biochim. Biophys. Acta* **1985**, *811*, 265.
[25] a) E. I. Solomon, R. G. Hadt, *Coord. Chem. Rev.* **2011**, *255*, 774; b) K. M. Clark, Y. Yu, N. M. Marshall, et al., *J. Am. Chem. Soc.* **2010**, *132*, 10093; c) M. A. Webb, C. N. Kiser, J. H. Richards, et al., *J. Phys. Chem. B* **2000**, *104*, 10915.
[26] B. G. Karlsson, M. Nordling, T. Pascher, et al., *Protein Eng.* **1991**, *4*, 343.
[27] Y. Y. Zhu, Y. Zhang, J. B. Zhan, et al., *FEBS Open Bio* **2019**, *9*, 986.
[28] A. E. Palmer, D. W. Randall, F. Xu, et al., *J. Am. Chem. Soc.* **1999**, *121*, 7138.
[29] a) M. Atanasov, D. Ganyushin, K. Sivalingam, et al., *Molecular Electronic Structures Of Transition Metal Complexes II. Structure And Bonding, Vol. 143* (Eds: D. Mingos, P. Day, J. Dahl), Springer, Berlin, Heidelberg **2012**, 149; b) T. J. Lawton, L. A. Sayavedra-Soto, D. J. Arp, et al., *J. Biol. Chem.* **2009**, *284*, 10174.
[30] J. Han, T. M. Loehr, Y. Lu, et al., *J. Am. Chem. Soc.* **1993**, *115*, 4256.
[31] a) N. A. Sieracki, S. L. Tian, R. G. Hadt, et al., *Proc. Natl. Acad. Sci. U. S. A.* **2014**, *111*, 924; b) C. J. Carrell, J. K. Ma, W. E. Antholine, et al., *Biochemistry* **2007**, *46*, 1900.
[32] D. K. Garner, M. D. Vaughan, H. J. Hwang, et al., *J. Am. Chem. Soc.* **2006**, *128*, 15608.
[33] J. Szuster, U. A. Zitare, M. A. Castro, et al., *Chem. Sci.* **2020**, *11*, 6193.
[34] a) B. L. Vallee, R. J. P. Williams, *Proc. Natl. Acad. Sci. U. S. A.* **1968**, *59*, 498; b) J. A. Guckert, M. D. Lowery, E. I. Solomon, *J. Am. Chem. Soc.* **1995**, *117*, 2817.
[35] T. P. Silverstein, *J. Chem. Educ.* **2012**, *89*, 1159.
[36] a) H. J. Wijma, I. MacPherson, O. Farver, et al., *J. Am. Chem. Soc.* **2007**, *129*, 519; b) M. D. Harrison, C. Dennison, *ChemBioChem* **2004**, *5*, 1579; c) S. Yanagisawa, C. Dennison, *J. Am. Chem. Soc.* **2005**, *127*, 16453.
[37] O. Farver, N. M. Marshall, S. Wherland, et al., *Proc. Natl. Acad. Sci. U. S. A.* **2013**, *110*, 10536.
[38] O. Farver, P. Hosseinzadeh, N. M. Marshall, et al., *J. Phys. Chem. Lett.* **2015**, *6*, 100.
[39] A. Romero, C. W. G. Hoitink, H. Nar, et al., *J. Mol. Biol.* **1993**, *229*, 1007.
[40] a) M. M. Bradford, *Anal. Biochem.* **1976**, *72*, 248; b) S. Stoll, A. Schweiger, *J. Magn. Reson.* **2006**, *178*, 42; c) A. Meents, B. Reime, N. Stuebe, et al., *Proc. SPIE 8851, X-Ray Nanoimaging: Instruments and Methods, 88510K*, **2013**, 10.1117/12.2027303; d) A. Burkhardt, T. Pakendorf, B. Reime, et al., *Eur. Phys. J. Plus* **2016**, *131*, 1; e) W. Kabsch, *Acta Crystallogr. Sect. D. Biol. Crystallogr.* **2010**, *66*, 125; f) P. R. Evans, G. N. Murshudov, *Acta Crystallogr. Sect. D. Biol. Crystallogr.* **2013**, *69*, 1204; g) A. J. McCoy, R. W. Grosse-Kunstleve, P. D. Adams, et al., *J. Appl. Crystallogr.* **2007**, *40*, 658; h) M. D. Winn, C. C. Ballard, K. D. Cowtan, et al., *Acta Crystallogr. Sect. D. Biol. Crystallogr.* **2011**, *67*, 235; i) P. Emsley, K. Cowtan, *Acta Crystallogr. Sect. D. Biol. Crystallogr.* **2004**, *60*, 2126; j) A. Immirzi, In *Crystallographic Computing Techniques* (Ed: F. R. Ahmed), Munksgaard, Copenhagen, **1966**, p. 399; k) G. N. Murshudov, P. Skubák, A. A. Lebedev, et al., *Acta Crystallogr. Sect. D. Biol. Crystallogr.* **2011**, *67*, 355; l) V. B. Chen, W. B. Arendall, J. J. Headd, et al., *Acta Crystallogr. Sect. D. Biol. Crystallogr.* **2010**, *66*, 12; m) A. E. Palmer, R. K. Szilagyi, J. R. Cherry, et al., *Inorg. Chem.* **2003**, *42*, 4006; n) L. L. C. Schrödinger, https://pymol.org/, **2015**.

Manuscript received: September 30, 2024
Accepted manuscript online: November 14, 2024
Version of record online: November 25, 2024